Near-Unity Anisotropic Infrared Absorption in Monolayer Black Phosphorus With/Without Subwavelength Patterning Design

Naixing Feng, *Member, IEEE*, Jinfeng Zhu, *Senior Member, IEEE*, Chawei Li, Yuxian Zhang, *Student Member, IEEE*, Zhengying Wang, Zhongzhu Liang, and Qing Huo Liu, *Fellow, IEEE*

***Abstract*—As an emerging anisotropic two-dimensional (2-D) material, few-atomic-layer black phosphorus (BP) has shown some promising potentials for infrared optoelectronics. Engineering and enhancing its light-matter interaction is significant for many advanced photonic devices. In view of this, we aim to achieve extremely high infrared absorption in monolayer BP with/without subwavelength patterning. By optimizing the polarization and angle of the incident light, the dielectric thickness, and the *n*-type doping concentration, respectively, infrared radiation can be sufficiently coupled to optical absorption of the monolayer BP in a multiscale photonic structure. The anisotropic infrared absorbance ratios of the unpatterned monolayer BP are enhanced up to 98.2% and 96%, respectively, in inequivalent crystal directions. Moreover, monolayer BP with a design of metasurface and optimized doping can reach near-unity anisotropic infrared absorption under a smaller incident angle. This paper provides a simple and efficient scheme to trap infrared light for developing promising optoelectronic devices based on monolayer BP and potentially other anisotropic 2-D materials.**

***Index Terms*—Anisotropic media, absorbing media, optical materials, phosphorus.**

Manuscript received May 16, 2018; revised October 24, 2018; accepted December 19, 2018. Date of publication December 24, 2018; date of current version January 4, 2019. This work was supported in part by the National Nature Science Foundation of China under Grant U1830116, in part by the Shenzhen Science and Technology Innovation Committee under Grant JCYJ20170306141755150, in part by the Guangdong Natural Science Foundation under Grant 2018A030313299, and in part by the Fujian Provincial Department of Science and Technology under Grant 2017J01123 and Grant 2015H0039. *(Corresponding authors: Jinfeng Zhu and Qing Huo Liu.)*

N. Feng is with the Institute of Electromagnetics and Acoustics, and the Department of Electronic Science, Xiamen University, Xiamen 361005, China, with the Shenzhen Research Institute of Xiamen University, Shenzhen 518057, China, and also with the College of Electronic Science and Technology, Shenzhen University, Shenzhen 518060, China (e-mail: fengnaixing@gmail.com).

J. Zhu, C. Li, Y. Zhang, and Z. Wang are with the Institute of Electromagnetics and Acoustics, and the Department of Electronic Science, Xiamen University, Xiamen 361005, China, and also with the Shenzhen Research Institute of Xiamen University, Shenzhen 518057, China (e-mail: nanoantenna@hotmail.com; xmucwlee@163.com; yxzhang_tute@126.com; zywang@stu.xmu.edu.cn).

Z. Liang is with the State Key Laboratory of Applied Optics, Changchun Institute of Optics, and Fine Mechanics and Physics, Chinese Academy of Sciences, Changchun 130033, China (e-mail: liangzz@ciomp.ac.cn).

Q. H. Liu is with the Department of Electrical and Computer Engineering, Duke University, Durham, NC 27708 USA (e-mail: qhliu@duke.edu).

This paper has supplementary downloadable material available at http://ieeexplore.ieee.org, provided by the authors. This includes a PDF containing information relevant to the paper. This material is 559 KB in size.

Color versions of one or more of the figures in this paper are available online at http://ieeexplore.ieee.org.

Digital Object Identifier 10.1109/JSTQE.2018.2889423

I. Introduction

AS WELL known in the advanced materials community, the angstrom-scale two dimensional layered materials (2DLMs) [1], [2] have attracted a tremendous amount of interests from condensed matter physicists, chemists, semiconductor device engineers, and material scientists, because they have great promise for applications in photonics [3]–[9], electronics [10]–[18], thermoelectrics [19], 20], and sensing [21], [22]. Each monolayer in 2DLMs, such as graphene, hexagonal boron nitride, transition metal dichalcogenides (TMDs), is weakly bounded to adjacent mono-layers by van der Waals (vdW) forces, so they are also called vdW materials. The vdW materials show almost all optical properties found in their 3D counterparts, such as optical resonances because of oscillations of surface plasmon polaritons, and light emission/lasing and excitons generated in semiconductors [23]. In addition to this, they possess extraordinary optical characteristics which are affected by material dimensionality and topology, and have boosted the development of advanced optics from nano-optics to angstrom-optics. Numerous theoretical and experimental studies about the interaction between light and 2DLMs, such as polaritons, wave guiding and confinement, have been continuously pushed forward on account of opportunities for novel devices [24]–[29]. Along with this research process, new modeling and simulation methods are much in demand to optimize the designs of 2DLMs-based photonic devices. In most of the related designs, vdW materials are usually incorporated with conventional 3D geometrical bulk structures, which might introduce a multiscale computational problem in simulation, require massive CPU time and memory, and make the optimization process tiresome. In order to overcome this problem, the surface current density method can be applied by treating 2DLMs as conductive surface boundaries [30], rather than extremely thin 3D effective medium layers, to yield not only tremendous computation efficiency, but also exceptional simulation consistency with experimental results.

Black phosphorus (BP), as an emerging member of 2DLMs, has been introduced into the 2D material family, which exhibits high carrier mobility, strong light-matter interaction in the mid- and far-infrared range, and high degree of band anisotropy [31], [32]. Particularly, BP is distinct from graphene and TMDs in the electronic band structure due to its remarkable direct band

gap strongly depending on the number of atomic layers, which covers the range from ∼0.3 eV for bulk BP to ∼2.0 eV for a monolayer form, and this makes it a critical supplement between graphene and TMDs for 2D optoelectronics [33], [34]. Very recently, BP has been studied for potential applications including field effect transistors [5], [10], [14], [15], heterojunction p-n diode [6], photovoltaic devices [7], and photodetectors [3]. Different from graphene and TMDs with in-plane isotropy, the BP shows in-plane anisotropic properties because of a unique puckered layered atomic structure, in which there are two inequivalent geometrical directions: the armchair edge (perpendicular to the atomic ridges) and the zigzag edge (parallel to the atomic ridges). The Raman scattering spectra and photoluminescence measurements for BP have revealed its highly anisotropic properties in experiments [35]. Some theoretical papers have implied anisotropic polaritons in mono or few-layer BP originated from different effective masses along distinct crystal in-plane directions [36]. Z. Liu *et al.* have theoretically demonstrate localized surface plasmon resonances (LSPR) of monolayer BP subwavelength nanoribbon and nanopatch arrays at the infrared range, and indicated BP's remarkable anisotropic plasmonic responses due to its puckered crystal structure [37]. The polariton effects indicate that BP is a promising 2D plasmonic material for angstrom-optics [38]–[41], which has capabilities of light confinement and electromagnetic field localization at deep subwavelength scales. In spite of these contributions, the reported infrared absorption ratio of two dimensional BP materials, especially monolayer BP, are still relatively low, which hinders its further applications in practical photonic devices. Therefore, an efficient and cost-effective method for light trapping in BP is still quite in demand for reaching higher infrared absorption in BP.

By systematic studies in this paper, we propose a method to achieve near-unity infrared absorption in a monolayer BP material by manipulating the polarization and angle of incident light, the thickness of dielectric layer and the n-type doping concentration. This method uses a simple 3D photonic structure incorporating a monolayer BP with/without subwavelength patterning. In these structures, the BP monolayer is separated from a metallic mirror by a dielectric spacer layer. In view of existing multiscale problems in computational electromagnetics, we use the finite element method (FEM) simulations in combination with the technique of surface current boundary, which treats the vdW material as a 2D surface described by the physical parameter of conductivity, rather than an extremely thin 3D bulk in numerical simulations. Mathematical analysis based on the coupling mode theory (CMT) is also performed and used as a comparison for a better explanation of the physics [42]–[45]. Based on the conditions of CMT, the influencing factors originated from the dielectric layer, BP anisotropy and n-type doping concentration, incident angle and polarization are comprehensively discussed and optimized for extremely high optical absorption in BP. Additionally, BP monolayer with subwavelength patterning is investigated, and also shows extremely high near-unity infrared absorption. The subwavelength patterning structure and n-type doping concentration are optimized for high infrared absorption with a smaller incident angle.

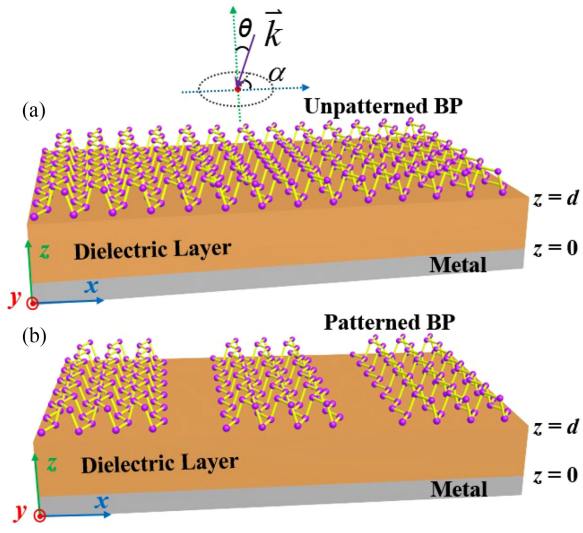

Fig. 1. (a) Proposed structure with unpatterned BP, where the armchair and zigzag directions are along the x axis and y axis, respectively. (b) Patterned BP for LSPR excitation. The symbols α and θ represent the azimuth and elevation angles of incident light, respectively.

II. Formulation

As an analogue to graphene, the thickness of few-atomic-layer BP is much smaller than the infrared wavelength, and its photonic properties can properly be depicted by in-plane anisotropic optical conductivities, which can be described by the semiclassical Drude model as below [36],

$$\sigma_j(\omega) = i \cdot \frac{D_j}{\pi\left(\omega + i\eta/\hbar\right)} \tag{1}$$

where

$$D_j = \sum_k \frac{\pi e^2 n_k}{m_j^k}, m_{cx}^k = \frac{\hbar^2}{2\gamma^2/(E_c^k - E_\nu^k) + \eta_c}, m_{cy}^k = \frac{\hbar^2}{2\nu_c}$$

As shown in the above, D_j is the Drude weight, j denotes x or y directions, k denotes the number of subbands [36], E_c^k and E_ν^k are the conduction and valence band edge energies, and m_{cx}^k and m_{cy}^k are in-plane electron effective masses along the x (armchair) and y (Zigzag) directions, respectively, as shown in Fig. 1(a). In order to depict this photonic property of monolayer BP, we take the first subband with an energy gap $\Delta = 2$ eV, the coupling parameter $\gamma = 4a/\pi$ eVm, the fitting parameters of effective masses $\eta_c = \hbar^2/(0.4m_0)$ and $\nu_c = \hbar^2/(1.4m_0)$, where $\hbar$ is the reduced Plank constant, m_0 is the electron mass, $\alpha = 0.223$ nm and π/a is the width of Brillouin Zone in the x direction [36], [37]. For monolayer BP, at the temperature of 300 K, the intrinsic electron concentration $n_1 = 10^{13}$ cm^{-2} and the relaxation rate $\eta = 10$ meV are used for the Drude model.

Here, we propose and investigate a simple 3D bulk structure incorporating monolayer BP, as shown in Fig. 1(a). In order to achieve extremely high infrared absorption, we adopt and deduce a unique critical coupling mode model for 2D materials with in-plane anisotropy. In this model, the dielectric and mirror layers are assumed as a lossless material and a perfect conductor, respectively. Based on a conventional critical coupling mode theory, the infrared light from free space can be

coupled and trapped in the proposed layered photonic structure by a certain resonance due to the optical reflection from its top and bottom surfaces. The infrared trapping efficiency is correlated with the external decay rate γ_e radiation through the top surface and the internal absorption decay rate γ_i in BP. When the critical coupling condition $\gamma_e = \gamma_i$ is satisfied, complete infrared absorption can be obtained. $\gamma_e = \gamma_i$ can be manipulated by the polarization and angle of incident light. In the proposed structure, BP monolayer is atomically thin and only the incident light with its electric field parallel to the BP surface is capable of interacting with this 2D material and dissipating to optical loss. Therefore, only *s*-polarized incident light has the potential possibility to achieve complete infrared absorption, so we mainly focus on the analysis discussion of *s*-polarized light.

Initially, we start from studying the general optical response of the layered photonic structure without BP, as shown in Fig. 1(a). In terms of the light wave impedance match conditions and the continuity of transverse components of the electromagnetic fields at the air-dielectric interface, the reflection coefficient can be obtained due to the fact that the impedance has to be continuous across the interface between the air interface for the air side and the air interface for the dielectric side [42], as shown below,

$$r = \frac{1 - i\left(\omega - \omega_0\right)\frac{d}{c}\cdot\frac{\varepsilon - \sin^2\theta}{\cos\theta}}{1 + i\left(\omega - \omega_0\right)\frac{d}{c}\cdot\frac{\varepsilon - \sin^2\theta}{\cos\theta}} \tag{2}$$

where c is the light speed, ω_0 is angular frequency of resonance, and d is thickness of dielectric layer. Next, the CMT is adopted to re-express the reflection coefficient [42]–[45], as shown below,

$$\frac{S_-(\omega)}{S_+(\omega)} = \frac{1 - i\left(\omega - \omega_0\right)/\gamma_e}{1 + i\left(\omega - \omega_0\right)/\gamma_e} \tag{3}$$

where S_+ and S_- represent the amplitudes of incoming and outgoing waves, respectively. It can be observed from eq. (2) and eq. (3) that both of the two equations are for the reflection coefficient and equivalent, hence we can derive the external decay rate below,

$$\gamma_e = \frac{c\cdot\cos\theta}{d(\varepsilon - \sin^2\theta)} \tag{4}$$

Next, we calculate the internal decay rate in the presence of a BP monolayer atop the dielectric structure. The internal decay rate due to the absorption in BP material is calculated by $\gamma_i = E_{BP}/E_d$, where the total energy within the dielectric resonant structure is shown below,

$$\begin{aligned} E_d &= \frac{1}{2}\int_0^d dz\left[\varepsilon_r\varepsilon_0|E(\omega)|^2 + \mu_r\mu_0|H(\omega)|^2\right] \\ &= \frac{1}{2}\varepsilon_r\varepsilon_0 d|CE_0|^2 \end{aligned} \tag{5}$$

E_{BP} describes the energy dissipation inside the BP material, which can be expressed as below,

$$\begin{aligned} E_{BP} = \frac{Re(\sigma)}{2}|E(\omega)_{z=d}|^2 &= \frac{Re(\sigma_y)}{2}|CE_0\cos\alpha|^2 \\ &+ \frac{Re(\sigma_x)}{2}|CE_0\sin\alpha|^2 \end{aligned} \tag{6}$$

where σ_x and σ_y are electrical conductivities for *x*- and *y*-direction, respectively, E_0 is the original excitation field, and C is the auxiliary coefficient used to simplify the expression. Indeed, because monolayer BP is atomically thick, it typically maintains the field distribution inside the structure. Therefore, the internal decay rate, which is due to absorption in a BP material separated from a PEC by a lossless spacer in *s*-polarization, is equal to the structure with BP material atop this structure, so we have

$$\gamma_i = \frac{Z_0 c}{d\varepsilon_r}\cdot\left(Re(\sigma_y)|\cos\alpha|^2 + Re(\sigma_x)|\sin\alpha|^2\right) \tag{7}$$

where Z_0 is the wave impedance of free space, and the relative permeability μ_r is equal to 1 because BP is non-magnetic.

As seen γ_e in (4) and γ_i in (7), it can be found that the *c*/*d* is the common item, so that we can substitute and tidy up equation (4) into equation (7), as shown below,

$$\begin{aligned} A = &\frac{Z_0\cdot\left[\left(Re(\sigma_y)|\cos\alpha|^2 + \mathrm{Re}(\sigma_x)|\sin\alpha|^2\right)\right]}{\varepsilon_r} \\ &\cdot\left(\cos\theta + \frac{\varepsilon_r - 1}{\cos\theta}\right) \end{aligned} \tag{8}$$

where A represents the optical absorption in monolayer BP, in terms of the different combinations of α and θ for *s*-polarized light. In order to reach complete infrared absorption in monolayer BP, A should equal to 1. Hence, we can solve this equation to find out the critical angle θ_c for extremely high absorption. Here, we replace $\sin^2\theta$ to $1 - \cos^2\theta$, adopt some mathematical approximation discussed in the Supporting Information, and simplify the expression for critical angle, as shown below,

$$\theta_c \approx \frac{\pi}{2} - \begin{cases} \frac{\varepsilon_r - 1}{\varepsilon_r}\cdot Z_0\mathrm{Re}(\sigma_x) \\ \frac{\varepsilon_r - 1}{\varepsilon_r}\cdot Z_0\mathrm{Re}(\sigma_y) \end{cases} \tag{9}$$

Based on the calculated infrared conductivities of monolayer BP in Fig. 2(a), both $Z_0\mathrm{Re}(\sigma_x)$ and $Z_0\mathrm{Re}(\sigma_y)$ are very close to zero, so the critical angle can be calculated and it is estimated to be close to 90°.

III. Simulation Results

As mentioned above, we have theoretically demonstrated and derived the expression based on the CMT, which can be utilized to determine the critical coupling angles for achieving extremely high infrared absorption in unpatterned BP monolayers. To further demonstrate the advantages of proposed method versus the scheme based on plasmonic excitation, we compare the infrared absorbance ratios for unpatterned and patterned BP monolayer materials, as shown in Fig. 2(b) and (c). It is observed that the infrared absorbance ratios in patterned BP monolayers by optimized plasmonic excitation under *p*-polarized light are only about 26% and 5% for electric field along *x* and *y* directions, respectively. In contrast, for unpatterned BP monolayers, near-unity infrared absorption can be achieved by gradually increasing the incident angle from 30° to the critical angle under *s*-polarized light incidence, regardless of the electric field along *x* or *y* directions. Besides, the full wave at half maximum (FWHM) for unpatterned BP monolayer under critical

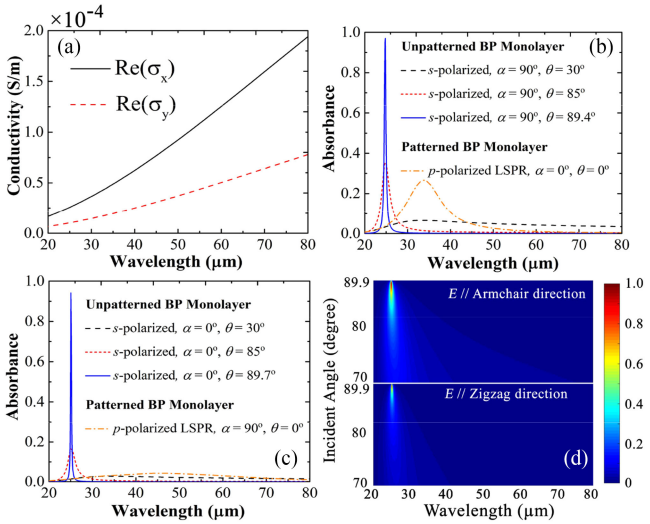

Fig. 2. (a) The real part of the anisotropic optical conductivity of BP monolayer in the armchair (σ_x) and zigzag (σ_y) directions. (b) Absorbance ratios for the electric field along the armchair direction. (c) Absorbance ratios for the electric field along the zigzag direction. A 4.6 μm-thick dielectric spacer layer with the refractive index of 1.7 is adopted, and the period and BP width for the patterned structure are 250 nm and 150 nm, respectively. (d) Anisotropic infrared absorption of unpatterned BP monolayer under *s*-polarized light, as a function of wavelength and incident angle.

coupling is extremely narrow (only 0.437 μm and 0.219 μm for x and y directions, respectively). Compared with the FWHM of 9.713 μm and 37.888 μm for x and y directions in patterned BP monolayer by LSPR excitation, the critical coupling scheme indicates much better selection property of absorption wavelength. Additionally, the central absorption wavelength and maximum absorption by critical coupling on the unpatterned BP monolayer are much less dependent on its anisotropy of conductivity, which is also further indicated in Fig. 2(d). This property sufficiently eliminates the discrepancy of anisotropy for near unity infrared absorption in the monolayer BP.

The mechanism of light-BP interaction is further revealed in Fig. 3(a) and (b). Based on our previous work [46], the optical loss in 2D materials is mainly induced by the in-plane electric field. The electric field for any incident angle of *s*-polarized light is parallel to the BP monolayer surface under *s*-polarized light illumination, but only the electric field under critical coupling is extremely enhanced. As shown in Fig. 3(a) and (b), for both electric fields parallel to armchair and zigzag directions, the field amplitudes under their critical angles (89.4° and 89.7°, respectively) are much larger than under the angle of 30°. This can be further explained by the optical coupling between the light waves from the lower and upper interfaces of alumina. Under the critical angles, the electric field on the surface of monolayer BP is maximized, and the in-plane anisotropic absorption ratios of BP monolayer reach the largest values for the armchair (98.2%) and zigzag (96%) directions, respectively. In addition, we also illuminate the critical angle coupling conditions for maximum absorbance at various central wavelengths by tuning the thickness of alumina layer (not shown in this figure). Analytical results of CMT are compared with FEM simulation results in Fig. 3(c) and (d), which indicate good agreement, and imply the route to narrow-band complete infrared absorption at

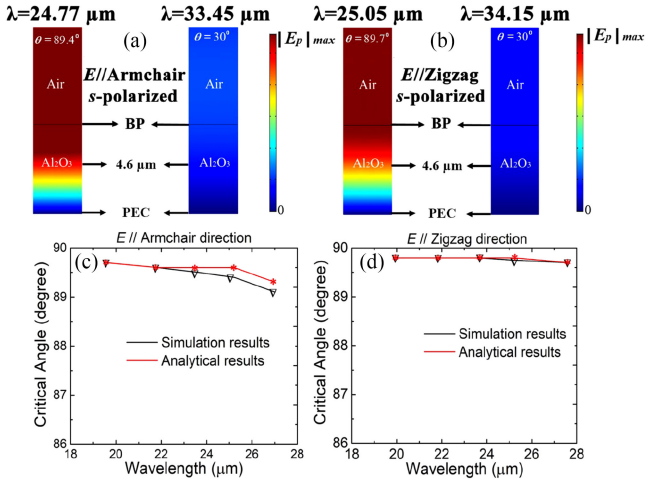

Fig. 3. Electric field distributions of the unpatterned stucture for *s*-polarized light under 30° and critical angle incidence with the electric field along (a) armchair direction and (b) zigzag direction, respectively, where $|E_p|$ denotes the amplitude of the electric field component parallel to the BP monolayer surface. Critical angles of anisotropic maximum absorbance ratios at various central wavelengths with optimized alumina thicknesses, for the electric field along (c) armchair direction and (b) zigzag direction respectively.

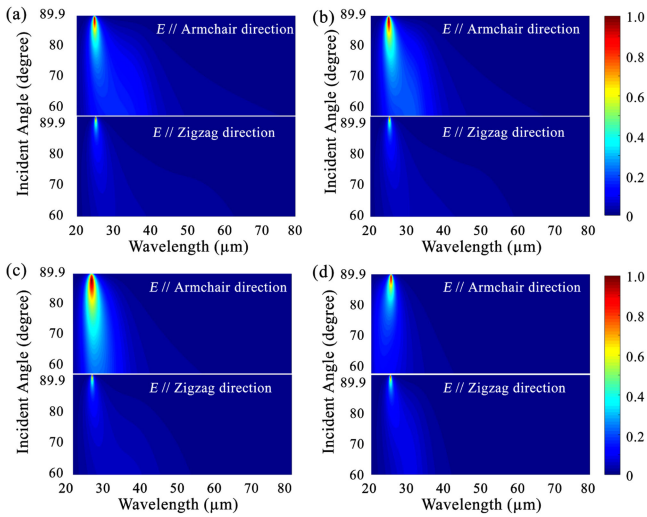

Fig. 4. Anisotropic infrared absorbance of BP monolayer under *s*-polarized light, as a function of wavelength and incident angle. The thickness of alumina layer is 4.6 μm, and the duty ratio of the square holes are (a) 2/5, (b) 12/25, (c) 3/5, and (d) 19/25, respectively.

different wavelengths. As shown in Fig. 3(c), the analytical results have small deviations from the simulation results, especially in longer wavelengths. This is because the analytical results are approximated based on a small optical conductivity, but this approximation is weakened as the conductivity increases in the armchair direction.

We next study the robustness of the proposed method on the condition of having various subwavelength square nanoholes (i.e., metasurface) on the BP monolayer. BP monolayers with subwavelength square holes of various sizes are taken into account, and their angle-dependent anisotropic optical properties are shown in Fig. 4. To simplify our investigation, periodic boundary conditions with a period of 250 nm are used, and the duty ratios between the length of square nanohole and the

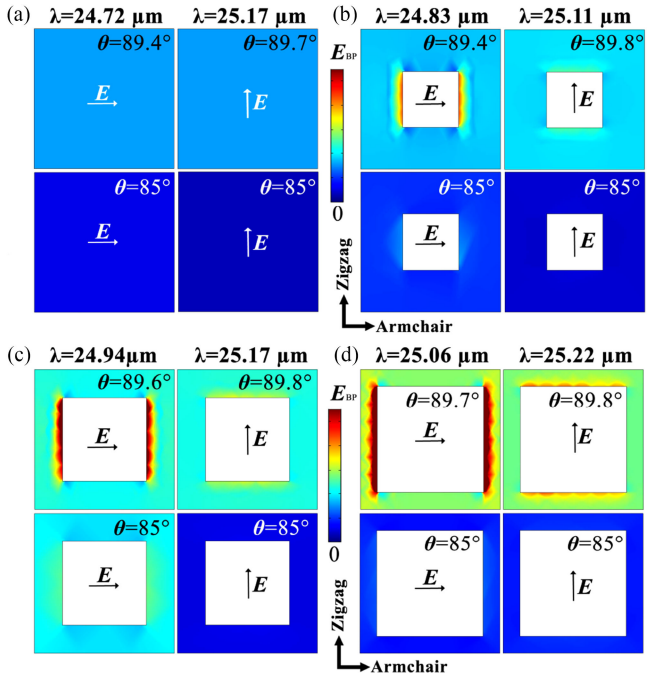

Fig. 5. Anisotropic energy distributions on monolayer BP surface under corresponding critical angles and 85°. (a) Unpattern BP monolayer, and patterned BP monolayer with the duty ratio of (b) 2/5, (c) 3/5, and (d) 19/25 respectively.

period are 2/5, 12/25, 3/5 and 19/25, respectively (see Fig. S2 in the supplementary material). As shown in Fig. 4, the near unity infrared absorption in monolayer BP with nanoholes of different sizes can still be achieved based on critical coupling for electric fields along zigzag and armchair directions, and the central wavelengths of absorption bands for various hole sizes change slightly, which demonstrates the reliability and stability of the proposed scheme. Fig. 4 also shows that the change of hole size influences the FWHM of the absorption band and the range of incident angle for critical coupling, especially for the condition of electric field along the armchair direction. For a certain hole size (i.e., the duty ratio of 3/5), the absorption band becomes wider and more incident angles satisfy critical coupling for extremely high absorption.

Furthermore, we reveal the physics of critical coupling by investigating the in-plane anisotropic energy distributions of BP monolayer surface with/without square nanoholes, as illustrated in Fig. 5. The in-plane energy distributions are calculated based on eq. (6). As shown in Fig. 5(a), the in-plane energy distributions on unpatterned BP monolayer are uniform under the conditions of critical angles, which are 89.4° and 89.7° for armchair and zigzag directions, respectively. When the incident angles deviate the critical coupling conditions and keep at 85°, the energy decreases significantly, especially for the zigzag direction with a smaller optical conductivity. For patterned BP monolayers, there are strong in-plane anisotropic dipole resonances under the critical coupling conditions. In view of the hole period of deep subwavelength, the dipole resonances are induced by the electric field. The critical angles increase slightly as the size of hole becomes larger (from Fig. 5(b) to Fig. 5(d)), which can be explained by the reduction of an effective optical conductivity for monolayer BP, as shown in equation (9).

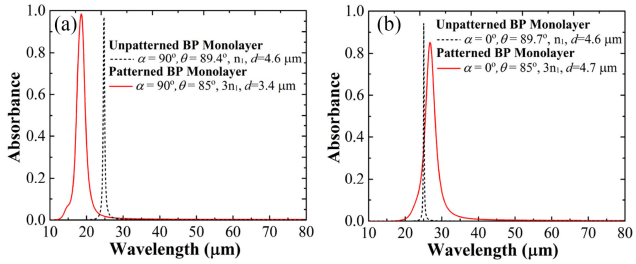

Fig. 6. Near-unity anisotropic infrared absorbance for unpatterned and patterned BP monolayers under *s*-polarized light illumination. (a) Electric field along the armchair direction. (b) Electric field along the zigzag direction. The symbol n_1 denotes the n-type doping concentration of BP monolayer.

The extremely high anisotropic absorption in patterned BP is attributed to the critical coupling as well as the mode of dipole resonance. The energy dissipation on BP surface is determined by not only the anisotropic infrared conductivities but also the duty ratios. When the incident angles are changed to 85°, the dipole modes are significantly weakened for duty ratios of 2/5 and 19/25, as observed in Fig. 5(b) and Fig. 5(d), respectively. For an optimum duty ratio of 3/5, the dipole mode for the armchair direction in Fig. 5(c) is still maintained with a relatively high energy density on the BP layer, which is also originated from a higher optical conductivity in the armchair direction.

With the aim of achieving extremely high infrared absorption in unpatterned BP monolayers, one should use an incident angle close to 90°, which might be too large and difficult in practical implementation. Based on the analysis in Fig. 5, one can use a smaller incident angle by adopting the patterned BP with an optimized structure and increased optical conductivities by n-type doping. By using 3 times of electronic doping with a duty ratio of 3/5, an incident angle of 85° can be applied for near-unity infrared absorption, as shown in Fig. 6(a) and Fig. 6(b). The near-unity infrared absorbance ratios of 98.4% and 85.2% are achieved in the armchair and zigzag directions, respectively, which are comparable with the maximum absorbance ratios of unpatterned structure. Compared with the patterned structure under critical coupling, the anisotropic absorption bands are broadened and have a spectral shift due to the change of the thickness of alumina. The near-unity infrared absorption is due to the critical coupling and dipole resonance of a patterned structure with a higher n-type doping. These results demonstrate that one can achieve extremely high anisotropic absorption by optimizing the nanostructure in combination with increasing the n-type doping, because there is a limitation for higher doping concentration in 2D materials.

IV. Discussions and Conclusions

In conclusion, based on the anisotropic properties of BP monolayer, we derive the mathematical expression for its extremely high infrared absorption by the theory of critical coupling theory, and further provide the physical insight by using finite element simulations. The unpatterned and subwavelength-patterned BP monolayers are investigated and compared. In addition to the critical coupling theory, a mode of dipole resonance is illuminated for the extremely high infrared absorption in a patterned structure. We perform a systematic study on the effects of

dielectric layer thickness, n-type doping, duty ratio of nanoholes and incident angles. The near-unity absorption is reached in not only the unpatterned structure but also the patterned structure by tuning these parameters. The monolayer BP with subwavelength square nanoholes and optimized doping can achieve near unity infrared absorption under a smaller incident angle. This research pave the way for developing high-performance photonic devices with strong infrared-BP interaction, and also provides an efficient method to trap infrared light for other 2D materials and related devices.

REFERENCES

[1] A. Castellanos-Gomez, "Why all the fuss about 2D semiconductors?," *Nat. Photon.*, vol. 10, pp. 202–204, 2016.

[2] X. Ling, H. Wang, S. Huang, F. Xia, and M. S. Dresselhaus, "The renaissance of black phosphorus," *Proc. Nat. Acad. Sci. USA*, vol. 112, pp. 4523–4530, 2015.

[3] M. Engel, M. Steiner, and P. Avouris, "Black phosphorus photodetector for multispectral, high-resolution imaging," *Nano Lett.*, vol. 14, pp. 6414–6417, 2014.

[4] T. Low, M. Engel, M. Steiner, and P. Avouris, "Origin of photoresponse in black phosphorus phototransistors," *Phys. Rev. B*, vol. 90, p. 081408, 2014.

[5] M. Buscema *et al.*, "Fast and broadband photoresponse of few-layer black phosphorus," *Nano Lett.*, vol. 14, pp. 3347–3352, 2014.

[6] Y. Deng *et al.*, "Black phosphorus-monolayer MoS2 van der Waals heterojunction p-n diode," *ACS Nano*, vol. 8, pp. 8292–8299, 2014.

[7] M. Buscema, D. J. Groenendijk, G. A. Steele, H. S. J. van der Zant, and A. Castellanos-Gomez, "Photovoltaic effect in few-layer black phosphorus PN junctions defined by local electrostatic gating," *Nat. Commun.* vol. 5, .2014, Art. no. 4651.

[8] T. Hong *et al.*, "Polarized photocurrent response in black phosphorus field-effect transistors," *Nanoscale*, vol. 6, pp. 8978–8983, 2014.

[9] J. Zhu, Q. H. Liu, and T. Lin, "Manipulating light absorption of graphene using plasmonic nanoparticles," *Nanoscale*, vol. 5, pp. 7785–7789, 2013.

[10] L. Li *et al.*, "Black phosphorus field-effect transistors," *Nat Nanotechnol.*, vol. 9, pp. 372–377, 2014.

[11] F. Xia, H. Wang, and Y. Jia, "Rediscovering black phosphorus as an anisotropic layered material for optoelectronics and electronics," *Nat. Commun.*, vol. 5, 2014, Art. no. 4458.

[12] H. Liu *et al.*, "Phosphorene: An unexplored 2D semiconductor with a high hole mobility," *ACS Nano*, vol. 8, pp. 4033–4041, 2014.

[13] S. P. Koenig, R. A. Doganov, H. Schmidt, A. H. C. Neto, and B. Özyilmaz, "Electric field effect in ultrathin black phosphorus," *Appl. Phys. Lett.*, vol. 104, 2014, Art. no. 103106.

[14] H. Wang *et al.*, "Black phosphorus radio-frequency transistors," *Nano Lett.*, vol. 14, pp. 6424–6429, 2014.

[15] Y. Du, H. Liu, Y. Deng, and P. D. Ye, "Device perspective for black phosphorus field-effect transistors: Contact resistance, ambipolar behavior, and scaling," *ACS Nano*, vol. 8, pp. 10035–10042, 2014.

[16] S. M. Kim *et al.*, "Transparent and flexible graphene charge-trap memory," *ACS Nano*, vol. 6, pp. 7879–7884, 2012.

[17] Q. H. Wang, K. Kalantar-Zadeh, A. Kis, J. N. Coleman, and M. S. Strano, "Electronics and optoelectronics of twodimensional transition metal dichalcogenides," *Nat. Nanotechnol.*, vol. 7, pp. 699–712, 2012.

[18] S. Das *et al.*, "Tunable transport gap in phosphorene," *Nano Lett.*, vol. 14, pp. 5733–5739, 2014.

[19] G. Qin *et al.*, "Hinge-like structure induced unusual properties of black phosphorus and new strategies to improve the thermoelectric performanc," *Sci. Rep.*, vol. 4, 2014, Art. no. 6946.

[20] R. Fei *et al.*, "Enhanced thermoelectric efficiency via orthogonal electrical and thermal conductances in phosphorene," *Nano Lett.*, vol. 14, pp. 6393–6399, 2014.

[21] L. Kou, T. Frauenheim, and C. Chen, "Phosphorene as a superior gas sensor: Selective adsorption and distinct I-V response," *J. Phys. Chem. Lett.*, vol. 5, pp. 2675–2681, 2014.

[22] J. Y. Wang, Y. Li, Z. Y. Zhan, T. Li, L. Zhen, and C. Y. Xu, "Elastic properties of suspended black phosphorus nanosheets," *Appl. Phys. Lett.*, vol. 108, 2016, Art. no. 013104.

[23] Y. Liu, N. O. Weiss, X. Duan, H. Cheng, Y. Huang, and X. Duan, "Van der Waals heterostructures and devices," *Nat. Rev. Mater.*, vol. 1, 2016, Art. no. 16042.

[24] D. N. Basov, M. M. Fogler, and F. J. Garcia de Abajo, "Polaritons in Van der Waals materials," *Science*, vol. 354, pp. 1–8, 2016.

[25] Y. Cai *et al.*, "Enhanced spatial near-infrared modulation of graphene-loaded perfect absorbers using plasmonic nanoslits," *Opt. Express*, vol. 23, pp. 32318–32328, 2015.

[26] A. Y. Nikitin, P. Alonso-Gonza´lez, and R. Hillenbrand, "Efficient coupling of light to graphene plasmons by compressing surface polaritons with tapered bulk materials," *Nano Lett.*, vol. 14, pp. 2896–2901, 2014.

[27] Y. Cai, J. Zhu, and Q. H. Liu, "Tunable enhanced optical absorption of graphene using plasmonic perfect Absorbers," *Appl. Phys. Lett.*, vol. 106, 2015, Art. no. 043105.

[28] J. Chen *et al.*, "Optical nano-imaging of gate-tunable graphene plasmons," *Nature*, vol. 487, pp. 77–81, 2012.

[29] V. W. Brar, M. S. Jang, M. Sherrott, J. J. Lopez, and H. A. Atwater, "Highly confined tunable mid-infrared plasmonics in graphene nanoresonators," *Nano Lett.*, vol. 13, pp. 2541–2547, 2013.

[30] J. Zhu, J. Cheng, L. Zhang, and Q. H. Liu, "Modeling of 2D graphene material for plasmonic hybrid waveguide with enhanced near-infrared modulation," *Mater. Lett.*, vol. 186, pp. 53–56, 2017.

[31] X. Wang and S. Lan, "Optical properties of black phosphorus," *Adv. Opt. Photon.*, vol. 8, pp. 618–655, 2016.

[32] D. Correas-Serrano, J. S. Gomez-Diaz, A. A. Melcon, and A. Alù, "Black phosphorus plasmonics: Anisotropic elliptical propagation and nonlocality-induced canalization," *J. Opt.*, vol. 18, 2016, Art. no. 104006.

[33] J. Wang and Y. Jiang, "Infrared absorber based on sandwiched two-dimensional black phosphorus metamaterials," *Opt. Express.*, vol. 25, pp. 5206–5216, 2017.

[34] A. Castellanos-Gomez, "Black phosphorus: Narrow gap, wide applications," *J. Phys. Chem. Lett.*, vol. 6, 2015, Art. no. 4280.

[35] S. Zhang *et al.*, "Extraordinary photoluminescence and strong temperature/angle-dependent raman responses in few-layer phosphorene," *ACS Nano*, vol. 8, pp. 9590–9596, 2014.

[36] T. Low *et al.*, "Plasmons and screening in monolayer and multilayer black phosphorus," *Phys. Rev. Lett.*, vol. 113, 2014, Art. no. 106802.

[37] Z. Liu and K. Aydin, "Localized surface plasmons in nanostructured monolayer black phosphorus," *Nano Lett.*, vol. 16, pp. 3457–3462, 2016.

[38] A. Nemilentsau, T. Low, and G. Hanson, "Anisotropic 2D materials for tunable hyperbolic plasmonics," *Phys. Rev. Lett.*, vol. 116, 2016, Art. no. 066804.

[39] S. A. Maier, "Plasmonics: Fundamentals and Applications," New York, NY, USA: Springer-Verlag, 2007.

[40] L. I. Berger, "Semiconductor Materials," Boca Raton, FL, USA: CRC Press, 1996.

[41] J. S. Gomez-Diaz and A. Alu´, "Flatland optics with hyperbolic metasurfaces," *ACS Photon.*, vol. 3, pp. 2211–2224, 2016.

[42] L. Zhu *et al.*, "Angle-selective perfect absorption with two-dimensional materials," *Light-Sci. Appl.*, vol. 5, 2016, Art. no. e16052.

[43] H. A. Haus, W. P. Huang, S. Kawakami, and N. A. Whitaker, "Coupled-mode theory of optical waveguides," *J. Lightw. Technol.*, vol. 5, no. 1, pp. 16–23, Jan. 1987.

[44] W. Suh, Z. Wang, and S. Fan, "Temporal coupled-mode theory and the presence of non-orthogonal modes in lossless multimode cavities," *IEEE J. Quantum Elect.*, vol. 40, no. 10, pp. 1511–1518, Oct. 2004.

[45] S. Fan and W. Suh, "Temporal coupled-mode theory for the Fano resonance in optical resonators," *J. Opt. Soc. Amer. A.*, vol. 20, pp. 569–572, 2003.

[46] J. Zhu, S. Yan, N. Feng, L. Ye, and Q. H. Liu, "Near unity ultraviolet absorption in graphene without patterning," *Appl. Phys. Lett.*, vol. 112, 2018, Art. no. 153106.

Naixing Feng (S'16–M'18) received the B.S. degree in electronic science and technology and the M.S. degree in microelectronics and solid-state electronics from Tianjin Polytechnic University, Tianjin, China, in 2010 and 2013, respectively, and the Ph.D. degree from the College of Electronic Science and Technology, Xiamen University, Xiamen, China, in 2018. From 2015 to 2016, he studied and was a Visiting Scholar supported by the CSC with the Department of electrical and computation engineering, Duke University, Durham, NC, USA. He is currently an Associate Professor with the College of Electronic Science and Technology, Shenzhen University, Shenzhen, China. He has appeared around 40 papers published by refereed international journals and conferences. His current research interests include computational electromagnetics and acoustics, photonic and nanomaterials and their applications.

Jinfeng Zhu (M'15–SM'17) received the B.S. degree in electronic communication science and technology and the Ph.D. degree in physical electronics from the University of Electronic Science and Technology of China, Chengdu, China, in 2006 and 2012, respectively. From November 2009 to November 2011, he was a Visiting Researcher with the Device Research Laboratory and Department of Electrical Engineering, University of California, Los Angeles, CA, USA. Since July 2012, he has been with Xiamen University, Xiamen, China, where he is currently an Associate Professor of electrical engineering. From July 2017 to July 2018, he was a Visiting Scholar with the Optoelectronics Research Centre, University of Southampton, Southampton, U.K. He has authored or coauthored more than 60 peer-reviewed journal and conference papers. His research interests include nanoantennas, nanophotonics, plasmonics, metamaterials, and Van der Waals materials.

Chawei Li received the B.S. degree from Huazhong University of Science and Technology, Wuhan, China, in 2016. He is currently working toward the M.S. degree in electromagnetic field and microwave technology from Xiamen University, Xiamen, Fujian, China. His research interests include nanomicro optoelectronic devices based on two-dimensional materials.

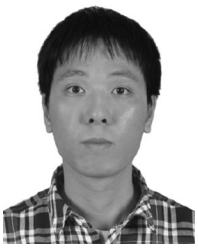

Yuxian Zhang (S'16) received the B.S. and M.S. degrees from Tianjin University of Technology and Education, Tianjin, China. He is currently working as a postgraduate student toward the Ph.D. degree in radio physics at Xiamen University, Xiamen, China. His main work is to implement the subsurface electromagnetic imaging in the reverse-time migration method. His current research interests include computational electromagnetics in the time-domain algorithm. He has authored or coauthored 21 papers in refereed journals and conference proceedings. He was the recipient of Chinese National Scholarship for three times and participated in Chinese Graduate Mathematical Contest in Modeling for five times with national awards.

Zhengying Wang received the B.S. degree in electronic science and technology in 2013 from Xiamen University, Xiamen, China, where she is currently working as a postgraduate student toward the M.S. degree in electronics and communication engineering. Her research interests include nanophotonics and microfluidics.

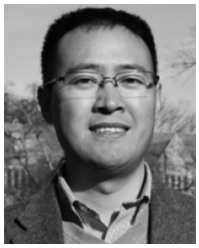

Zhongzhu Liang received the B.S. degree from the College of Materials Science and Engineering, Jilin University, Changchun, China, in 2002, and the Ph.D. degree from State Key Laboratory of Superhard Materials, Jilin University, China, in 2007 majored in the synthesis and optical characterization of the diamond with nitrogen impurities. From December 2013 to January 2015, he was a Visiting Scholar with the Electrical and Computer Engineering, Duke University, under the financial support from the China Scholarship Council. He was a Professor with the State Key Laboratory of Applied Optics, Changchun Institute of Optics, Fine Mechanics and Physics, Chinese Academy of Sciences in September, 2014. He has authored and coauthored more than 90 peer-reviewed journal and conference papers. His research interests include micro-optical electromechanical-system, plasmonics and sensors.

Qing Huo Liu (S'88–M'89–SM'94–F'05) received the B.S. and M.S. degrees in physics from Xiamen University, Xiamen, China, in 1983 and 1986, and the Ph.D. degree in electrical engineering from the University of Illinois at Urbana-Champaign, Champaign, IL, USA, in 1989.

His current research interests include computational electromagnetics and acoustics, inverse problems, and their applications in geophysical subsurface sensing, biomedical imaging, and nanophotonics. He has authored or coauthored more than 450 papers in refereed journals and 500 papers in conference proceedings. He was with the Electromagnetics Laboratory, University of Illinois at Urbana-Champaign, Champaign, IL, USA, as a Research Assistant from September 1986 to December 1988, and as a Postdoctoral Research Associate from January 1989 to February 1990. He was a Research Scientist and a Program Leader with Schlumberger–Doll Research, Ridgefield, C, USA, T from 1990 to 1995. From 1996 to May 1999, he was an Associate Professor with New Mexico State University. Since June 1999, he has been with Duke University, Durham, NC, USA, where he is currently a Professor of Electrical and Computer Engineering.

Dr. Liu is a Fellow of the Acoustical Society of America, Electromagnetics Academy, and the Optical Society of America. He is currently the founding Editor-in-Chief for the IEEE JOURNAL ON MULTISCALE AND MULTIPHYSICS COMPUTATIONAL TECHNIQUES, the Deputy Editor in Chief of *Progress in Electromagnetics Research*, an Associate Editor for the IEEE TRANSACTIONS ON GEOSCIENCE AND REMOTE SENSING, and an Editor for the *Journal of Computational Acoustics*. He was the recipient of the 1996 Presidential Early Career Award for Scientists and Engineers from the White House, the 1996 Early Career Research Award from the Environmental Protection Agency, the 1997 CAREER Award from the National Science Foundation, and the 2017 Technical Achievement Award from the Applied Computational Electromagnetics Society. He was with the IEEE Antennas and Propagation Society Distinguished Lecturer in 2014–2016.